

REVIEW PAPER

Airborne Infrared Search and Track Systems

Hari Babu Srivastava¹, Y.B. Limbu, Ram Saran, and Ashok Kumar

¹*Instruments Research and Development Establishment, Dehradun-248 008*

ABSTRACT

Infrared search and track (IRST) systems are required for fighter aircraft to enable them to passively search, detect, track, classify, and prioritise multiple airborne targets under all aspects, look-up, look-down, and co-altitude conditions and engage them at as long ranges as possible. While the IRST systems have been proven in performance for ground-based and naval-based platforms, it is still facing some technical problems for airborne applications. These problems arise from uncertainty in target signature, atmospheric effects, background clutter (especially dense and varying clouds), signal and data processing algorithms to detect potential targets at long ranges and some hardware limitations such as large memory requirement to store and process wide field of view data. In this paper, an overview of airborne IRST as a system has been presented with detailed comparative simulation results of different detection/tracking algorithms and the present status of airborne IRSTs.

Keywords: IRST, FLIR, thermal imaging, false alarm rate, wavelet transform, FOV, infrared search and track systems, airborne IRST systems, field of view, forward-looking infrared, target tracking

1. INTRODUCTION

Infrared search and track (IRST) systems are wide field of view surveillance systems, designed for autonomous search, detection, tracking, classification and prioritisation of potential targets, passively. IRST systems¹ are becoming more and more important in air defence applications because radars do not meet the requirement of passive surveillance, suffer from jamming, and are vulnerable to anti-radiation missiles. Other reason for preference of IRST systems over radars is dramatic increase in IR sensor performance, resulting in long-range detection capability. The IRST systems are getting more and more importance in air defence applications due to increased reluctance to use radar sensors because of threat of anti-radiation missiles and dramatic increase in IR sensor performance. On the other

hand, however, targets are becoming less and less observable and the requirement of user are becoming more and more stringent; e.g., larger field of view (FOV), detection against dense and complex backgrounds with target entering from all directions with high speeds, detection of point target at very long ranges, etc. In addition, IRST should be able to provide landing and flying-aid capability during night and bad weather conditions.

The technologies involved in the IRST systems are similar to those used in thermal imaging systems and forward-looking infrared (FLIR) systems but have a difference². Thermal imaging systems are used for obtaining high-resolution imagery within specified FOVs, usually small, to detect, recognise and track potential targets at maximum possible range with human intervention. It uses line focal

plane arrays (LFPAs) (with mirrors to scan) or focal plane arrays (FPAs). FLIR is also an imaging system, whose output is an IR image of the forward scene. FLIRs are generally used for navigation and landing aid, but now these are also used for target cuing. The first- and second-generation IRSTs utilised detectors with multiple elements followed by discrete pre-amplifiers for signal read-out. With the advent of high-resolution large linear array IR sensors, the current IRSTs are able to form images and cover wide FOVs.

Number of questions arises during preliminary design/definition phase of IRST systems like choice of the use of IR wavelength (LWIR, i.e., 8-12 μm or MWIR, i.e., 3-5 μm), scanning/staring system, detector parameters like f number, etc.

Comparing MWIR with LWIR automatically includes different detectors with different quantum efficiencies. The best system is one that meets the need of particular application. Atmospheric conditions have the largest influence on MWIR/LWIR selection. Whether MWIR transmittance³ is better than LWIR depends upon the relationship between visibility and the water vapour concentration in the atmosphere.

2. SYSTEM REQUIREMENTS

Some of the operational requirements of IRST systems were discussed above. In the air-to-air scenario, some of the targets may be having high dynamics, while others may be having slow dynamics.

The clutter is generally a slow moving cloud background. Noise is present, apart from other reasons, due to fluctuating atmospheric transmission.

While operating in all the above scenarios, the detection rate should be very high (of the order of 95 %) and at the same time, false alarm rate should be very low. The IRST system should be able to track single as well as multiple targets and passively calculate range of the selected target using kinematics-ranging calculations. The reasons for using kinematics ranging calculations are: (i) it is able to give range information while target is beyond the scope of active range devices like laser range finder (LRF), (ii) using LRF, capable of ranging very long distant targets, the weight of the system increases which is a constraint for airborne applications, and (iii) one gives away his own position and becomes vulnerable to detection by enemy, the very reason for which IRST is being preferred over radar.

3. FUNCTIONAL ARCHITECTURE

The IRST system typically consists of a scanning head along with its control electronics and an IRST computer. The scanning head consists of a top scanning mirror, an IR module, and a LRF. The IR detector output after suitable proximity processing circuitry is transferred to IRST computer for computation of detection and tracking algorithms. The LRF output and other commands is also to be transferred between the head and the IRST computer.

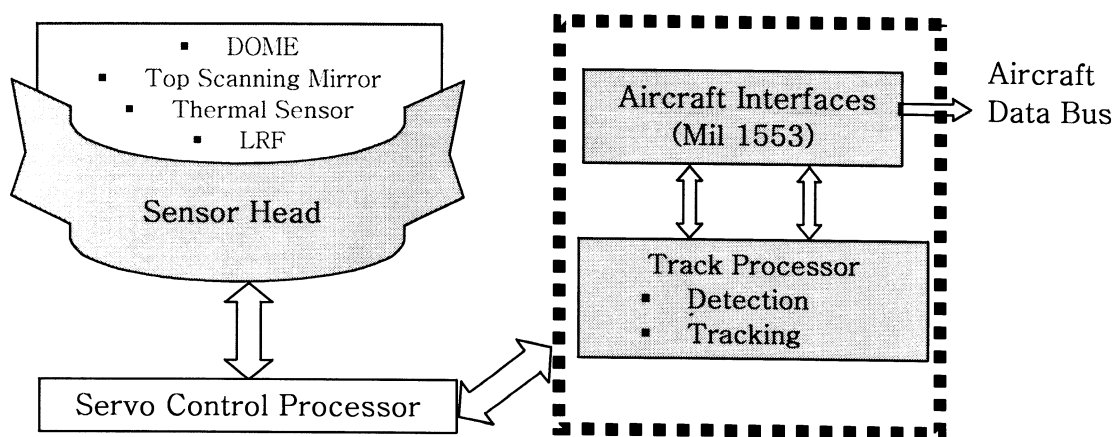


Figure 1. Infrared search and track system.

The IRST computer implements the algorithms for detection and tracking of airborne targets. The IRST computer interacts with weapon system computer on a digital bus like MIL bus 1553. Figure 1 shows the block diagram of an IRST system.

4. KEY PROBLEM AREAS

The IRST system is designed to detect targets at long ranges, which appear on image plane as point targets. In its simplest form, the atmospheric effect is illustrated using simple range formula for point target detection systems like IRST:

$$R = \sqrt{\frac{\Delta W * \tau(R)}{NEI * K}} \quad (1)$$

where, R is range, $\tau(R)$ is the atmospheric transmittance over the range R , ΔW the target radiant intensity contrast, NEI is the noise equivalent irradiance of the sensor, and K is the required signal-to-noise ratio for a given detection/false alarm probability.

One problem can be pointed out due to the fluctuations in background radiance, which does not have the same distribution as the target. But the variations in the background itself may also vary spectrally. For example, clouds; these sources change in position and shape in a rather slow pattern and edges of the clouds differ from cloud centres. Due to this, effective pre- and post-processing algorithms are needed to suppress the background clutter and enhance SNR of dim point targets.

Birds are also a potential source of false alarms in IRST systems. Signals generated by birds at

short ranges (1 - 2 km) in IR sensors may be of the same magnitude as the signals generated by real targets at longer ranges. Since IRST systems are based on scanning mechanism with very large FOVs and low frame rates (typically 0.5 - 3 frames/s), chances of false alarms due to birds flying at short distances increase, as the track build-up of the IRST is significantly slow.

The crux of the IRST system is the development of signal and data processing algorithms to detect point targets in a variety of scenarios. The details about various detection algorithms are given in the next section. The related issues also involve implementation of algorithms on hardware platforms and testing methodologies. While fast processors like PowerPC or high speed FPGA boards are available in the market, but to implement the detection algorithm based on temporal processing is still a problem due to large memory and computation power requirements. For example, in PIRATE (the IRST for Eurofighter TYPHOON)¹ the front-end data rate is 24 million pixels/s. To process this huge amount of data, large memory is required.

5. ELECTRO-OPTICAL SENSORS

An IRST scenario⁴ with the main sensor elements is given in the Fig. 2. A vertical detector array, positioned in the focal plane of the optical system, is scanned in the horizontal direction. The detector pixels are seen projected into object space. When the object space is scanned, target or background clutter signatures are mapped in to corresponding electrical signals.

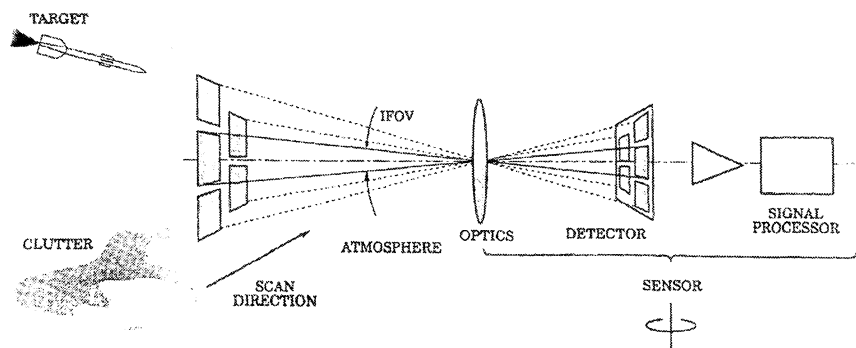


Figure 2. Infrared search and track system scenario.

The physical principles of electro-optical sensors and the principal components ofIRST are described in the following subsections.

5.1 Physical Principles

Unlike light, IR radiation is invisible to human beings because the wavelength is longer than the sensitivity range of the eye. The IR energy, like visible light, can be collected and focused onto a detector. Unlike light, it is emitted by all objects (temperature above 0 K) because of their internal heat. On the detector, the IR energy received is turned into electrical signal and finally to image through signal processing.IRST systems uses mid- and long-wavelength IR radiation because these occur naturally and are readily transmitted through the atmosphere. The objects in the scene are themselves the source of the radiation. The atmosphere limits the choice of wavelengths for IR systems to certain bands⁶ of the so called near, mid-wave, and long-wave IR. Surrounding these bands are wavelengths that are blocked by the atmosphere, through the interaction of gases and particles with the radiation. The degree of scattering in an atmosphere depends on the particle sizes present. Atmospheric particles are rarely bigger than 0.5 μm and so have little effect on wavelengths in excess of 3 μm . The haze or fog droplet size can be anything from 0.5 μm to 80 μm with the peak of their distribution being between 5 μm and 15 μm . Thus, fog particles are comparable to IR wavelengths and the atmospheric transmittance becomes poor. Three atmospheric windows define the usable regions of the IR referred to as near-, mid-, and far-IR.

5.2 Principal Components of anIRST System

The principal components of an IR system⁶ are the window, optics, cooler, electronics (signal and image processing systems) and display. TheIRST system typically consists of a scanning head along with its control electronics and anIRST computer. The scanning head consists of a top scanning mirror, an IR module, and a LRF. The IR detector output after suitable proximity processing circuitry are transferred toIRST computer. The LRF output and other commands are transferred between the head and theIRST computer.

Constructing anIRST system for defence applications generally requires rugged windows and housing to protect the equipment from the environment. These windows are made of IR transmitting materials such as germanium, zinc sulphide, and silicon. These have an important impact on system performance as their optical properties affect sensitivity and angular resolution directly. These windows have to be much stronger to support aerodynamic loads and resist erosion due to rain and sand as well as have suitable shape and position to avoid airframe drag.

The optical system is required to produce a focused image of a distant scene while eliminating radiation from sources outside the scene. Baffles are used to eliminate stray radiation inside the optical system. Filters are included to limit the range of wavelengths passed through the detector. Lenses and/or mirrors are used to collect and focus the radiation from the scene. Typically, a multi-element design is required so that optical aberrations can be minimised.

In general, an array of detectors is required, each staring at a particular region of the scene. Unless the array is sufficiently large, the total image is built up by scanning the scene across these detectors to produce a single frame. The scanning mechanism is required to map the instantaneous FOV to the FOV required in the scene.

The detector is the heart of any IR system. Its function is to absorb the IR radiation from the scene and convert it to an electrical signal. The strength of the signal is a measure of the temperature of that scene. Detectors devices are of two basic classes, thermal detectors and quantum detectors. Pyroelectrics is an important class of thermal detectors as these have the advantage of requiring no cooling, but these are slow to respond, if these are also required to be very sensitive. The detector material most employed in IR imaging system is cadmium mercury telluride (CMT) also referred to as MCT.

If the detector consists of a single or a small number of discrete elements, 2-D scanning will be required to compose a reasonable FOV. If one can

fill a whole column with detector elements, then 1-D scanning will make up the full field of view. Such detectors are popularly known as line-FPA (or LFPAs). If one has a full, 2-D array of detectors, one can remove the scanning process completely. Such detectors are known as area-FPA (or simply FPAs). An important procedure of time-delay integration is usually applied in IR detectors to increase their signal-to-noise ratio. An array of n detectors is used to sequentially visit the same region in object space. The output of these n detector columns is then integrated, which results in improvement of signal-to-noise ratio by \sqrt{n} . This process is known as time-delay integration (TDI). To ensure a uniform output from all detector elements for uniform input, disparities in sensitivity of individual detectors have to be corrected electronically. The serial scan detector, line-FPA and area-FPA (staring array)⁵ are presented in Fig. 3.

Quantum detectors require cooling in order that their response to IR radiation can be distinguished from electrical noise. As well as the detector device, it is also often necessary to cool a cold shield (an optical baffle that prevents thermal energy from equipment housing and optical system from entering the detector FOV). Different methods of cooling are used: Thermoelectric, Joule-Thomson, and Stirling cycle engine. Thermoelectric coolers exploit the

so called Peltier effect by which current flowing across a junction between dissimilar metals causes one metal to heat while the other to cool. Joule-Thomson cooler cools the detector assembly by expansion of a high pressure gas. By forcing the gas (usually nitrogen or argon) through narrow nozzle, it rapidly expands and in doing so, absorbs heat. Stirling cycle engines cool by mechanical refrigeration, i.e., by repeatedly compressing and expanding a gas.

5.3 Atmospheric for Infrared Systems

There are some basic processes by which the atmosphere affects IR radiation on its passage from the scene to the system⁵:

Absorption: Atmospheric gases in the path may absorb some of the radiation

Scattering: Atmospheric gases and suspended particles may scatter some radiation from the target out of the line-of-sight and some background radiation into the line-of-sight.

An empirical method for calculating the IR extinction was commonly used prior to the wide-scale dissemination of computer models for atmospheric effects. This method divides the IR spectrum up into eight windows. Then absorption and scattering are calculated separately for each window of interest, using empirical formulas.

5.3.1 Infrared Absorption

The point of view is adopted that the only variable component in atmospheric absorption is the amount of vapours. Other gases that may be absorbed in the IR range remain fairly constant in the concentration and therefore can have their effects incorporated in the constants of the algorithm. Computer-based algorithms use following empirical equations to get W :

$$x \equiv 273/T_A$$

$$W = 0.01.RH.x.R.\exp(18.9766 - 14.9545x - 2.4388x^2) \quad (2)$$

where, T_A is air temperature (K); RH is relative humidity (%); and R is range (km).

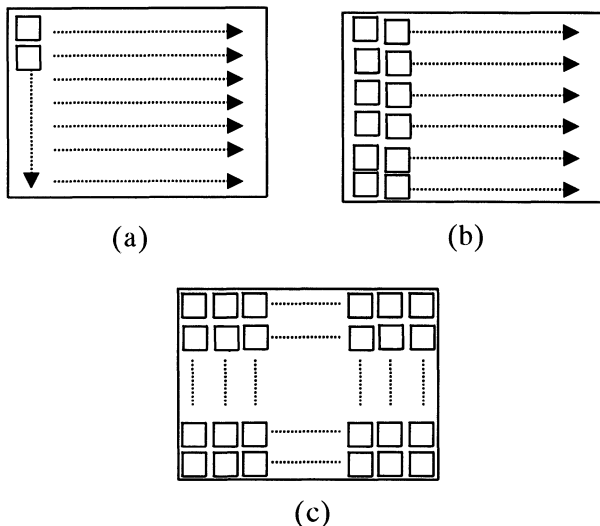


Figure 3. FLIR types: (a) Serial scan detector; (b) line-FLIR; (c) area-array FLIR.

The empirical expressions for absorption transmissivity in the i^{th} window at sea level are:

$$\tau_{ai} = \exp(-A_i W^{1/2}), \quad W < W_i \quad (3)$$

$$\tau_{ai} = k_i (W_i / W)^{\beta_i}, \quad W > W_i \quad (4)$$

If not at sea level, the transmissivity for a horizontal path can be approximated by

$$\tau_{ai}(h) = \tau_{ai}(\text{sea level}) \left[\frac{P(\text{sea level})}{P(h)} \right]^{0.25} \quad (5)$$

where h is altitude of horizontal path and PG is atmospheric pressure.

Slant paths would obviously be much more difficult, requiring some averaging process.

5.3.2 Infrared Scattering

The scattering transmissivity in the i^{th} window is approximately

$$\tau_{si} = \exp[-\beta(\lambda_i)R] \quad (6)$$

where, λ_i is the centre wavelength of the i^{th} window.

For Rayleigh scattering,

$$\beta_i(\lambda) = A\lambda^{-4}$$

However, pure Rayleigh scattering would represent very little loss. The main problem in IR scattering stems from the aerosols (large particles are suspended in the atmosphere).

At IR wavelengths

$$\beta_s = \frac{3.91}{V} \left(\frac{0.55}{\lambda} \right)^q \quad (7)$$

$$\tau_{si} = \exp \left[-\frac{3.91}{V} \left(\frac{0.55}{\lambda_i} \right)^q R \right] \quad (8)$$

In this algorithm, V first establishes q and then τ_{si} is calculated from the above equation.

The modelling of atmospherics is quite mature compared to most aspects of IR system modelling. LOWTRAN is a computer-based modelling tool that contains a number of models of atmosphere, stratified into 1 km layers up to 25 km above the sea level and into thicker layers from 25 km to 100 km. Furthermore, with the continuing refinement and release of updated versions of LOWTRAN, it will continue to be used as good atmospheric modelling tool.

5.4 Performance Modeling of IR Systems

There are some important performance measures for characterising the performance of the IR system as a whole⁵.

5.4.1 Noise-equivalent Temperature Difference

The performance measure for FLIR systems first is the noise-equivalent temperature difference (NETD). It is defined as the blackbody target-to-background temperature difference in a standard test pattern that produces a peak signal-to-rms-noise ratio of unity at the output of an electronic reference filter. The test pattern consists of a large square, uniform, hotter target on a uniform, cooler background. This square target should be at least several times larger than the system IFOV.

Under reasonable conditions the NETD⁵ is

$$NETD = \frac{\pi \sqrt{ab} \Delta \nu_R}{\alpha \beta A_E \tau_o D^*(\lambda_p) \frac{\Delta M}{\Delta T}} \quad (9)$$

$$\text{with } \frac{\Delta M}{\Delta T} \equiv \int \frac{\partial M_\lambda}{\partial T}(T_B) \frac{D^*(\lambda)}{D^*(\lambda_p)} d\lambda$$

where, a, b are the detector dimensions; α, β are the detector angular dimensions (IFOV); $\Delta \nu_R$ is the noise bandwidth of reference filter; A_E is the entrance pupil area; τ_o is the optics transmittance; $D^*(\lambda_p)$ is the peak spectral density; $D^*(\lambda)$ is the spectral density, and T_B is the background temperature.

The NETD is a single value rather than a curve and may be used for rough estimates of SNR from the FLIR for large targets. SNR is defined as

$$\text{SNR} \approx \Delta T / \text{NETD}$$

where ΔT is the received temperature difference.

5.4.2 Minimum Resolvable Temperature Difference

The most widely used IR system performance measure is minimum resolvable temperature difference (MRTD). This quantity is measured using a test pattern. Again, blackbody radiation is assumed from the hotter bars and cooler background. Starting from 0, the temperature difference is increased until the largest bar pattern can just be confidently resolved. This temperature difference becomes the MRTD value for that lowest spatial frequency. It can be defined as

$$\text{MRTD}(v_x) = \frac{3\text{NETD}\sqrt{\rho\beta v_x}}{\text{MTF}_s(v_x)\sqrt{t_e FR}} \quad (10)$$

where v_x is the spatial frequency in the x direction; MTFs are the system modulation transformation function (MTF); t_e is the eye integration time; FR is the frame rate; and p is the ratio converting displayed noise bandwidth to that effective.

5.4.3 Modulation Transformation Function

The MTF is perhaps the most basic system performance measure. It is often difficult even to prove the existence of such function for some of the systems.

6. SIGNAL AND IMAGE PROCESSING ALGORITHMS FOR IRST SYSTEMS

Raw IR data from the sensor head electronics is digitised to a 12/14-bit wide digital data stream. Non-uniformity correction of all detector channels is required to be carried out. This non-uniformity corrected data is sent to the IRST signal processor for implementing the detection algorithms, forming the image, tracking the targets or estimating/measuring the range of the target.

6.1 Pre- and Post-processing of Infrared Data

Pre-processing of incoming IR data is a necessary step in the detection of airborne targets. It has

experimentally been verified that the detection of dim point size targets in cluttered background is not possible without increasing the SNR by pre-processing of IR data. Similarly post-processing of IR data is required to reduce the false alarm rate of detection. The algorithms used in pre-and post-processing of IR data are described.

6.1.1 Pre-processing of Infrared Data

Most of the algorithms proposed in the literature could not detect targets having intensity differential of 20 or less (on 8-bit gray level) without pre-processing. A number of pre-processing algorithms have been suggested in literature like max-mean, max-median, and morphological filtering. Max-median filter preserves the edges of clouds and structural background. But it removes low-contrast point target also, which is a serious limitation. In this filter, an $N \times N$ window is run over an image. The value of N , which is fixed, may be chosen from 3 to 7 as a tuning parameter (higher value results in higher complexity) to real situation demands. Median is found for column and row vector and two diagonal vectors wrt center pixel of window. Next, the intensity value for the centre pixel of the window is replaced by a maximum of these median values found. For max-median filters, with $N \times N$ window, $I(x, y)$ is replaced by a value

$$\tilde{I}(x, y) = \max(\text{median}_1, \text{median}_2, \text{median}_3, \text{median}_4) \quad (11)$$

Mathematical morphology is widely used in the area of image processing as image filtering. Gray-scale opening and closing operations are carried out with gray-scale dilation and erosion.

6.1.2 Post-processing of Infrared Data

To make the detection scheme robust to clutter and noise, post-processing techniques are used. Generated binary image is segmented and then all the segments having size larger than a threshold are removed. From a segmented image, candidate target list is prepared and used for further processing. Linked list containing information about size and centroid location of each segment is maintained.

Local contrast is defined as

$$lc(x_n, y_n) = \left| I(x_n, y_n) - \frac{1}{s_i} \sum_{(x_m, y_m) \in A_f} I(x_m, y_m) \right|$$

$$A_f = \left\{ \begin{array}{l} (x_j, y_j) | (x_j, y_j) \in N_r(x_n, y_n) \\ (x_n, y_n) \neq (x_j, y_j) \end{array} \right\} \quad (12)$$

where (x_n, y_n) is candidate point target of interest. $I(x_n, y_n)$ is the gray level value of pixel at (x_n, y_n) . s_i is the size of neighbourhood window in terms of pixels and N_r is the neighbourhood window defined by a circle of radius r centered at (x_n, y_n) . This local contrast is compared with some threshold to validate the candidate target.

Candidate targets are accepted or rejected as per the following threshold criterion:

$$|I(x_n, y_n) - I(x_m, y_m)| < \varepsilon \text{ for } \forall (x_m, y_m) \in N_8(x_n, y_n),$$

$m \neq n$ where $N_8(x_n, y_n)$ is the eight-connected neighbours of (x_n, y_n) .

6.2 Detection of Targets

A number of approaches have been reported for detection and tracking of point targets, viz. 3-D match filtering (velocity filter, sequence hypothesis test, dynamic programming)⁷, high-order correlation⁸, wavelet transform^{9,10} and neighbouring encoding criteria¹¹, etc. A lot of work has been done in the area of wavelet-based detection, but its high computation and data storage requirement results in complex and large electronics. Other methods proposed also suffer from one problem or the other. For example, neighborhood-based algorithm has the limitation in detecting low-contrast targets. Modified motion analysis-based detection algorithm (developed by IRDE and yet to be published) is able to detect dim point target of large movement from frame to frame. It has less computation complexity as compared to wavelet-based algorithm and at the same time less memory requirement. Matched filter-based point targets detection algorithm¹² has been reported in the literature. A method to analyse the point target detection

algorithms is published¹³. An algorithm for tracking point targets in hyperspectral image sequences is proposed¹⁴. In addition to point target detection and tracking algorithm, passive ranging algorithm for prediction of target range has been reported¹⁵.

6.2.1 Pipeline Target Detection Algorithm

Pipeline target detection algorithm¹⁶ (PTDA) is addressed for the task of detecting and tracking pixel-sized targets from a time sequence of dynamic images of a high-noise environment. The trajectories of the moving targets are unknown, but assumed to be continuous and smooth. It uses the temporal continuity of the smooth trajectories of moving targets and is based on the spatial consistency of intensity of a temporal target trajectory within a finite time period. But, the disadvantage with this approach is that it works with only slow target movement, typically 1-2 pixels per frame. Moreover, computationally it is expensive for large image frame, since it forms a pipe for every pixel in the frame. Another problem with this method is that it is not able to track a target in case of occlusion caused by clouds over several frames. To track a target with large movement (say 20 pixels per frame), the window size needs to be increased, and hence, it leads to the following:

- False alarm due to increased search neighbourhood in continuity filtering algorithm (CFA)
- Consequently, taking centroid position of temporal window column (TWC) as a detected target position will not be correct
- Number of additions per pixel increase by $O(N^2)$ with increase in maximum detectable target movement (pipe size), where N is the number of pixels in a frame.

6.2.2 Modified Pipeline Target Detection Algorithm

To overcome limitations of PTDA, a modified pipeline algorithm for tracking multiple single-pixel targets with large motion (20 pixels) in an IR image with occlusion due to IR clouds and background noise has been presented¹⁰.

In this method, constant acceleration Kalman filter is used to predict the position in next frame. A search window is formed around this predicted position. A pipe is formed at all pixels only inside the search window and not the whole frame. As will be seen later, this helps in handling large target motion (20 pixels), occlusion due to clouds, and binary noise.

Pipeline algorithm consists of two major components:

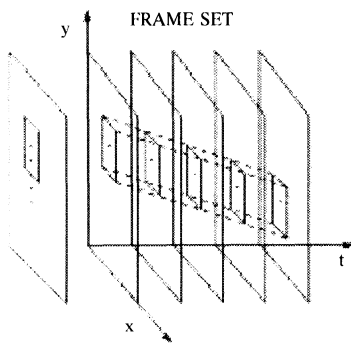
- (i) Fixed-length TEST PIPE of temporally adjacent image frames. At each iteration, a frame from the bottom of the test pipe is discarded and new frame is added to top of the pipe and other frames are shifted in pipe by one position.
- (ii) AND PIPE (AP) consists of two image frames and a single blank frame called target frame (TF). The CFA uses the AND PIPE to test continuity of the target pixel.

This algorithm is able to track fast moving targets, but fails if the target is maneuvering.

6.2.3 Wavelet-based Detection Algorithm

Wavelet transform is widely used to give better time-frequency localization. At a given level k , the signal C^k , called approximation signal, is split up into two terms: A new approximation signal at a coarser scale C^{k+1} ,

$$C^{k+1}(i) = \sum_n H(n-2i)C^k(n) \quad (13)$$



Modified test pipe

and a signal coding the difference in the information D^{k+1} ,

$$D^{k+1}(i) = \sum_n G(n-2i)D^k(n) \quad (14)$$

where H and G are the filter coefficients.

Above operations provide temporal multiscale decomposition. A two-hypotheses likelihood ratio test is applied to validate temporal changes at each scale. Two competing hypothesis are compared: Hypothesis H_0 (no temporal change) and H_1 (temporal change).

$$\Psi^k(p) \geq \lambda \text{ for } H_0$$

$$\Psi^k(p) < \lambda \text{ for } H_1$$

λ is a threshold which may be inferred from tables of statistical laws and $\Psi^k(p)$ is defined below:

$$\Psi^k(p) = \frac{1}{2\sigma_k^2} \left[\frac{1}{N} \left(\sum_{i=1}^N D^k(p_i) \right)^2 + \frac{1}{\sum x_i^2} \left(\sum_{i=1}^N x_i D^k(p_i) \right)^2 + \frac{1}{\sum y_i^2} \left(\sum_{i=1}^N y_i D^k(p_i) \right)^2 \right] \quad (15)$$

$\Psi^k(p)$ follows χ^2 distribution with three DOF. In the above equation, N is the size of the window in terms of pixels centered at point p_i and (x_i, y_i) indicates the relative location of pixels wrt the centre of window. The value of N , which is fixed, may vary from 3 to 7 depending upon tuning required for real data. σ_k^2 is variance of the pixel intensity within the frame. These change detection maps are binary images containing the pixel intensities either 0 or 4095. From the simulation, it is found that wavelet-based detection algorithm is able to detect high contrast targets but is not suitable for dim-point targets.

The intensity differential (gray-scale value) between targets and background for simulated image sequences is calculated and data show that if intensity differential is below 80 (on 8-bit image frame), wavelet-based algorithm is not able to detect point targets.

6.2.4 Neighbouring Encoding-based Detection Algorithm

This algorithm includes two modules, namely region of interest (ROI) locating and contour extraction. In the former module, image-differencing technique is employed on consecutive images to generate rough candidates of targets appearing in the images. Next, a novel encoding technique is devised to effectively remove noise that usually severely affect the performance of system. By assuming noise to be Gaussian-distributed, it is deductively concluded that pixels surrounded by three or less than three non-zero neighbours need to be examined in a difference image. From this point of view, the method encodes every pixel and its neighbours and then builds a histogram to determine noise threshold in the difference image.

6.2.5 Modified Motion Analysis-based Detection Algorithm

In the modified motion analysis-based algorithm¹⁷, first morphological operations are carried out on the incoming IR data to improve SNR. Methods of entropy thresholding and conjunction functions, as proposed by Nengli Dong¹⁸, *et al.*, are integrated. Conjunction function-based algorithm has been suitably modified to take care of fast moving targets, an important limitation of the method proposed by Nengli Dong¹⁸, *et al.* This algorithm is able to detect point as well extended low contrast targets having frame-to-frame movements varying from nil to many tens of pixels.

Conjunction function can be defined as

$$d_{seq}(i, j) = \min[c * (I_{seq}(i + n_i, j + n_j) - I_{seq-1}(i, j))]$$

$n_i, n_j \in \chi$ denote adjacent domain of some pixel, and c is a coefficient.

The above conjunction function is applied on each pixel of image frame. Then thresholding is performed on the result of conjunction function.

6.3 Manoeuvring Target Tracking

Various tracking approaches have been explored to track manoeuvring targets. In the presence of

multiple targets, the algorithm needs to associate an observation to the track for update and prediction of the target state. Nearest-neighbour technique is widely used for data association.

6.3.1 Interactive Multiple Model

In target tracking application, apriori knowledge about the target motion is not available; it may be non-maneuvring or manoeuvring. Two tracking approaches namely, interactive multiple model (IMM) and multiple filter bank (MFB), have been proposed to track non-maneuvring or manoeuvring targets. The IMM algorithm uses multiple models that interact through state mixing to track a manoeuvring target. The IMM algorithm consists of a filter for each model of target motion. It evaluates model probability for each filter and each target.

The probabilities are used for mixing state estimates of the targets. An underlying Markov chain governs the model switching. But, the problem with IMM-based method is that it requires extra computations for model probability update, mix state initialisation, combined target state estimate along with state and its covariance update and prediction for each model. However, IMM provides smooth switchover among the models used for tracking.

6.3.2 Multiple Filter Bank

To reduce number of computations, a different tracking method was explored to track multiple point/extended targets using multiple filter bank. In this method, both filters in the filter bank update their states in parallel and only one filter will be considered as active filter for updating state vector. The filter bank consists of CA and EIA filters. In the proposed method, switchover between the filters in the bank is based on single-step decision logic, and consequently, it is computationally more efficient and performance-wise more robust. The predicted position given by the active filter is used to form a validation gate for data association. To determine active filter, single-step decision logic, based on innovation error measure, is used to switchover between the filters.

6.3.3 *Nearest-neighbour Data Association Technique*

In this method, the observation is associated to the existing track using innovation error measure. The data assignment is made based on minimum distance, i.e., minimum error measure value. The innovation error is a difference between the predicted and the observed position. The validation region (gate) is formed based on this innovation error. The innovations-based approach is simple and easy to implement, and is quite effective.

A validation gate (region) is formed as follows:

The state transition equation and measurement equation for Kalman filter are given by

Dynamic equation (state transition equation):

$$x(k+1) = F(k)x(k) + v(k) \tag{16}$$

where $x(k)$ is the state vector of position, velocity and acceleration at time instant k . $v(k)$ is a zero mean, white, Gaussian process noise with covariance matrix $Q(k)$.

Measurement equation:

$$z(k) = H(k)x(k) + w(k) \tag{17}$$

where $w(k)$ is zero mean, white, Gaussian measurement noise with covariance $R(k)$.

The current set of measurements Z^k , at time instant k , are validated using the validation gate. Validation gate is formed based on innovation error using the following procedure. The predicted measurement is given by

$$\hat{z}(k+1|k) = H(k+1)\hat{x}(k+1|k) \tag{18}$$

For true measurement at time $k+1$, conditioned upon Z^k , is assumed to be normally distributed,

$$p[z(k+1)|Z^k] = N[z(k+1); \hat{z}(k+1), s(k+1)] \tag{19}$$

where $Z^k = \{z(i), 0 \leq i \leq k\}$ is the set of measurement and $s(k+1)$ is the innovation covariance matrix defined as

$$s(k+1) = E[\tilde{z}(k+1|k)\tilde{z}'(k+1|k)|Z^k] \tag{20}$$

Based on this, the region $\tilde{V}(\xi)$ is defined in the measurement space where the measurement will be found with high probability:

$$\tilde{V}(\xi) = \{z: \tilde{z}^T(k+1)s^{-1}(k+1)\tilde{z}(k+1) \leq \xi\} \tag{21}$$

where, $\tilde{z}(k+1) = z(k+1) - \hat{z}(k+1|k)$ is the innovation and ξ is a parameter obtained from tables of the chi-square distribution with number of DOFs equal to the dimension of measurement.

7. SIMULATION RESULTS OF DETECTION/ TRACKING ALGORITHMS

The performance of detection and tracking algorithms has been simulated on various synthetic and real image sequences. Simulation results based on three-image sequences are presented here. Image sequence 1 contains three-point targets (two with straight trajectories and one with slow manueuvring) embedded in synthetic background. The detection and tracking result based on PTDA is shown in Fig. 4. The size of image frame for image sequence 1 is 1024 x 256 pixels. Image sequence 2 is the recorded real background embedded with two-point



Figure 4. Image sequence 1: PTDA-based detection/tracking results.

targets (one with constant acceleration and the other one coordinated turn type of trajectory). The simulation result (detection based on wavelet-based algorithm and tracking based on IMM algorithm) is shown in Fig. 5. The size of image frame for image sequence 2 is 352 x 288 pixels. Image sequence 3 is real recorded clip with six targets. The size of the targets is varying from 2 pixels to 16 pixels, depending on the aspect angle. The size of the image frames is 500 x 332 pixels. Real image frame, wavelet-based detection, neighbouring encoding-based detection and modified motion analysis-

based algorithm (yet to be published) with MFB-based tracking are shown in Fig. 6. Both, wavelet and neighbouring encoding-based detection algorithms are not able to detect low-contrast targets. The reason is that the intensity differential between target and background goes below 20 (8-bit image) in this image sequence. Modified PTDA is suitable for straight trajectories and slow manoeuvring targets. Simulation study shows that wavelet-based detection algorithm may be a choice forIRST systems if sufficient target contrast is available (>80 gray-scale intensity differential on 8-bit image frame).

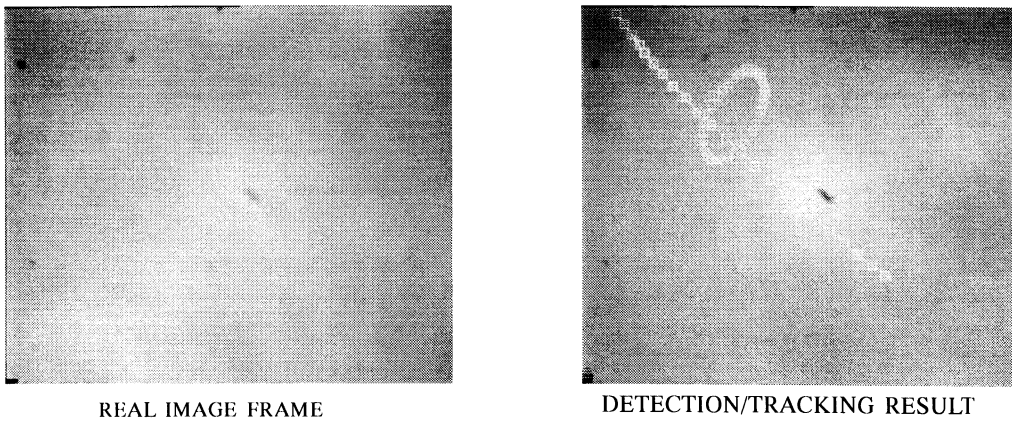


Figure 5. Image sequence 2: Wavelet-based detection with ID 80.

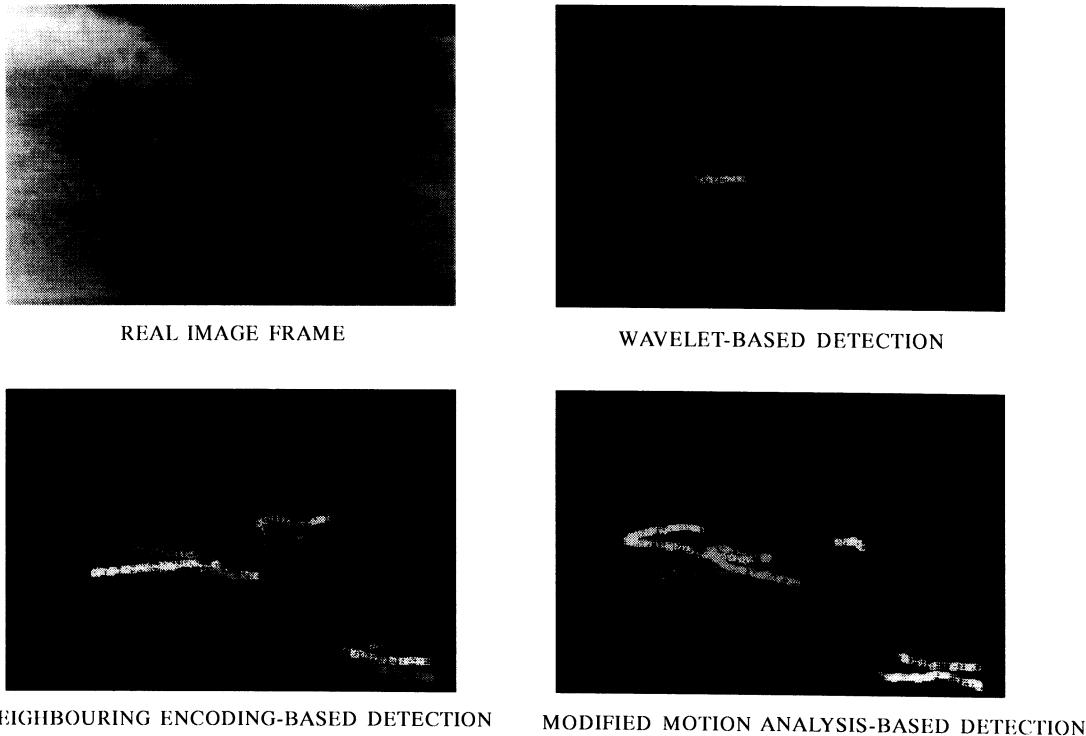


Figure 6. Image sequence 3: Detection/ tracking results.

Table 1. Summary of detection rate and false alarm rate using differential algorithms

| IR sequence | Probability of detection | | | Probability of false alarm | | |
|-------------------|--------------------------|------|------|----------------------------|------|------|
| | WBA | NBA | MMBA | WBA | NBA | MMBA |
| Seq_1 (Real) | 0.49 | 0.51 | 0.99 | 0 | 0 | 0.22 |
| Seq_2 (Real) | 0.05 | 0.41 | 0.83 | 0 | 0 | 0.03 |
| Seq_3 (Synthetic) | 0 | 0.94 | 0.99 | 0 | 0.04 | 0.07 |
| Seq_4 (Synthetic) | 0 | 0.97 | 1 | 0 | 0.07 | 0.08 |
| Seq_5 (Synthetic) | 0 | 0.97 | 1 | 0 | 0.06 | 0.08 |
| Seq_6 (Synthetic) | 0.18 | 0.98 | 0.98 | 0.01 | 0.03 | 0.06 |
| Seq_7 (Synthetic) | 0 | 0.98 | 1 | 0 | 0.18 | 0.10 |

WBA – Wavelet-based detection algorithm

NBA – Neighbourhood-based algorithm; MMBA - Modified motion-based detection algorithm

It fails as target contrast goes below the specified intensity differential. Modified motion analysis-based detection algorithm is able to detect point as well as extended size low-contrast targets. Modified pipeline algorithm has less computational load, but is not suitable for highly manoeuvring targets. The summary of detection rate and false alarm rate for experimented IR sequences is presented in Table 1.

The probability of detection and false alarm rate is calculated as shown in equations given below

$$\text{Detection Rate} = \frac{\text{Number of Correct Detection}}{\text{Total Number of Targets}} \quad (22)$$

$$\text{FalseAlarmRate} = \frac{\text{Number of False Detection}}{\left(\frac{\text{Number of Correct Detection} + \text{Number of False Detection}}{\text{Number of False Detection}} \right)} \quad (23)$$

8. COMPUTATIONAL COMPLEXITIES

The different algorithms have been implemented and the CPU time for frame size of 8885 x 480 pixels has been recorded. The algorithms were run on Intel Xeon processor running at 3.2 GHz. The source codes for different algorithms have been compiled using GNU gcc compiler. The source codes have lot of scope for optimization. The relative CPU time for different detection algorithms is given in Table 2.

High throughput and performance can be achieved by the COTS multiprocessor-based systems for

Table 2. Relating CPU time for different detection algorithms

| Algorithm | CPU time per frame (s) |
|---|------------------------|
| Wavelet-based algorithm | 17.51 |
| Neighbourhood-based algorithm | 1.62 |
| Modified motion-based detection algorithm | 17.36 |

real-time applications¹⁹ or through FPGA implementation of algorithms.

9. PRESENT STATUS

While many ground-based and naval platform-based IRSTs have been developed, airborne IRST systems are still under development. A survey of airborne IRSTs is presented.

9.1 Passive IR Airborne Track Equipment

Passive infrared airborne track equipment (PIRATE)²⁰ is totally passive multi-function track while scan sensor system. A consortium of European countries led by M/S Thales, UK, has developed this IR search and track system, known as PIRATE, for the Eurofighter Typhoon aircraft. It is single line replaceable unit (LRU). PIRATE has the claimed capability of long-range (up to 100 km) detection, tracking and prioritisation of multiple airborne



threats, high-resolution target and scene images. The quantitative figures for various performance parameters are not available in the published literature. It has been integrated with the weapon system of Eurofighter aircraft. At present, IRST flight-testing campaign and productionisation contract is in progress.

9.2 IR Optical Tracking and Identification System

Saab Bofors Dynamics, Sweden, has developed an IRST system named infrared optical tracking and identification system (IR-OTIS)²¹ and flight trials have been carried out with the system mounted on a Saab JAS39 Gripen fighter aircraft. IR-OTIS has mainly three operating modes:

IRST-mode—where the system covers several different FOS (field of search)

FLIR-mode (forward-looking IR)—where the systems LOS (line of sight) is directed from the aircraft

Track-mode—where the built-in-tracker controls the LOS. It is also possible to switch from IRST-mode to track-mode automatically.

A number of flight trials of this system have been reported. However, it is not clear from the published literature whether this system has been fully deployed on any aircraft or not. As with the PIRATE system, quantitative figures for various performance parameters are not available in the published literature.

9.3 AN/AAS-42 IRST

The F-14 AN/AAS-42 IRST is a passive long-wave IR sensor system that searches for and detects heat sources within its FOV. Operating in six discrete modes, the AN/AAS-42 provides the aircraft mission computer track file data on all targets while simultaneously providing IR imagery to the cockpit display. The AN/AAS-42 gives the aircrew unprecedented onboard situational awareness while significantly enhancing the engagement range of modern high-performance weapons such as the AIM-120 (AMRAAM). For this system also, quantitative figures for various performance parameters are not available in the published literature.

10. INDIAN SCENARIO

Some of the Indian aircraft have integrated IRST systems of the first generation. These operate in not so wide FOV (compared to the present generation IRSTs) and search/track single targets.

Instruments Research and Development Establishment (IRDE), Dehra Dun, has launched a programme to indigenously develop IRST system for deployment on Indian aircraft. This system is intended to give detection ranges up to 160 km under various operating conditions. The system will have the capability of track while scan feature and will be able to track multiple targets simultaneously.

11. CONCLUSIONS

IRST sensors, their physical principles and signal and image processing algorithms have been presented. The crux of IRST sensor is its signal processing algorithms. These systems require very high detection rate and very low-false alarm rate. High frame rate may result in highly improved processing algorithms to achieve such false alarm rate. The choice of detection algorithms depends on its versatility, the ability to work in a variety of scenarios with very high detection rate, and at the same time, very low false alarm. More accurate passive ranging algorithms are still the area of research and development.

ACKNOWLEDGMENTS

First and foremost, authors thank Shri J.A.R. Krishna Moorthy, Outstanding Scientist and Director IRDE, for his constant guidance and encouragement for carrying out the work reported here. The contributions of Prof U.B. Desai and Prof S.N. Merchant of IIT Bombay, Mumbai, and Prof Mukesh Zhaveri, NIT, Surat, are sincerely acknowledged. Authors also thank all the IRST team members who have directly or indirectly contributed towards this manuscript.

REFERENCES

1. Cook, Boyd. PIRATE—the IRST for Eurofighter TYPHOON. Infrared technology and applications. *Proceedings SPIE*, 2003, **4820**, 897-07.

2. Venkateswarlu, R.; Er, M.H.; Tam, S.C.; Chan, C.W. & Chao, L.C. Design consideration ofIRST system. *Infrared technology and applications, Proceedings SPIE*, 1997, **3061**, 591-02.
3. Holst, Gerald C. Common sense approach to thermal imaging. SPIE Optical Engineering Press, 2000. pp. 90-109.
4. Andreson, Bjorn F.; Ben-David, Itzhak; Glazer, Shlomo; Roth, Shmuel & Levy, Baruch. Surface-basedIRST: A selection process for sensor parameter values. *Proceedings SPIE*, 1997, **3061**.
5. Waldman, Gary & Wootton, John. Electro-optical systems performance modelling. ARTEC House, Inc, 1993.
6. Thermal imaging markets, Chap. 1: Technology and trends.
7. Cafer, Charlene E.; Silverman, Jerry & Mooney, Jonathan M. Optimisation of point target tracking filters. *IEEE Trans. Aero. Elect. Syst.*, 2000, **36**(1), 15-25.
8. New, W.L.; Er M.H. & Ronda, V. New method for detection of dim point-targets in infrared images. *Proceedings SPIE*, 1999, **3809**, 141-50.
9. Hewer, Gary; Kuo, Wei; Kenney, Charles; Hanson, Grant & Bobinchak, Jim. Detection of small IR objects using wavelets, matched subspace detectors, and registration. Signal and data processing of small targets. *Proceedings SPIE*, 2002, **4728**, 12-23.
10. Zaveri, Mukesh A.; Malewar, Anant; Merchant, S.N. & Desai, Uday B. Wavelet-based detection and modified pipeline algorithm for multiple point targets in infrared image sequences. *In ICVGIP*, 2002.
11. Hsieh, Feng-Yang; Han, Chin Chauan; Wu, Nai-Shen & Fan, Kuo-Chin. A novel approach to noise removal and detection of small objects with low contrast.
www.fox1.csie.ncu.edu.tw/~Synconph/paper/detection_wiamis04.pdf.
12. Buganim, S. & Rotman, S.R. Matched filters for multispectral point target detection. *Proceedings SPIE*, 2006, **6302**.
13. Adar, S.; Buganim, S. & Rotman, S.R. Analysing point target detection algorithms. *Proceedings SPIE*, 2005, **5987**.
14. Varsano, L. & Rotman, S.R. Point target tracking in hyperspectral images. *Proceedings SPIE*, 2005, **5806**, 503-10.
15. Visser, Maarten de; Schwering, Piet B.W.; de Groot, Johannes F. & Hendriks, Emile A. Passive ranging using an infrared search and track sensor. *Optical Engineering*, 2006, **45**(2).
16. Wang, Gang; Inigo, Rafael M. & McVey, Eugene S. A pipeline algorithm for detection and tracking of pixel-sized target trajectories. Signal and data processing of small targets. *Proceedings SPIE*, 1990, **1305**, 167-77.
17. Srivastava, Hari Babu; Saran, Ram & Kumar, Ashok. Modified motion-based algorithm for detection of dim point targets in IR image sequences. *Proceedings SPIE*, 2006, **6189**.
18. Dong, Nengli; Jin, Gang; Qi, Bo & Ma, Jianguang. New approach to detect dim moving point targets based on motion analysis. *In Signal and Data Processing of Small Targets. Proceedings SPIE*, 2001, **4473**, 34-42.
19. Cody, Robert F. & Ames, Kevin J. Achieving high throughput with COTS multicomputers: Infrared search and track case study. *Proceedings SPIE*, 1997, **3061**, 521-32.
20. Thales. Defence optronics systems, Air-to-air. <http://www.thales-optronics.com/>
21. Andersson, Ingmar & Leif Haglund. SAABIRST: The system and flight trails in Infrared Technology and Applications. *Proceedings SPIE*, 2000, **4820**, 69-83.